



HAL
open science

1,2-Dihydrophosphate: A Platform for the Molecular Engineering of Electroluminescent Phosphorus Materials for Light-Emitting Devices

Hui Chen, Simon Pascal, Zuoyong Wang, Pierre-Antoine Bouit, Zisu Wang, Yinlong Zhang, Denis Tondelier, Bernard Geffroy, Régis Réau, François Mathey, et al.

► To cite this version:

Hui Chen, Simon Pascal, Zuoyong Wang, Pierre-Antoine Bouit, Zisu Wang, et al.. 1,2-Dihydrophosphate: A Platform for the Molecular Engineering of Electroluminescent Phosphorus Materials for Light-Emitting Devices. *Chemistry - A European Journal*, 2014, 20 (31), pp.9784-9793. 10.1002/chem.201400050 . hal-01089789

HAL Id: hal-01089789

<https://univ-rennes.hal.science/hal-01089789v1>

Submitted on 23 May 2016

HAL is a multi-disciplinary open access archive for the deposit and dissemination of scientific research documents, whether they are published or not. The documents may come from teaching and research institutions in France or abroad, or from public or private research centers.

L'archive ouverte pluridisciplinaire **HAL**, est destinée au dépôt et à la diffusion de documents scientifiques de niveau recherche, publiés ou non, émanant des établissements d'enseignement et de recherche français ou étrangers, des laboratoires publics ou privés.

1,2-Dihydrophosphete: a new platform for the molecular engineering of electroluminescent P-materials for light-emitting devices

Hui Chen,^[b] Simon Pascal,^[a] Zuoyong Wang,^[b] Pierre-Antoine Bouit,^[a] Zisu Wang,^[b] Yinlong Zhang,^[b] Denis Tondelier,^[c] Bernard Geffroy,^[d] Régis Réau,^{*,[a]} François Mathey,^{*,[b]} Zheng Duan,^{*,[b]} Muriel Hissler,^{*,[a]}

Abstract: The discovery and molecular engineering of novel electroluminescent emitting materials is still a challenge in optoelectronics. In this work, we report on the development of new π -conjugated oligomers incorporating a dihydrophosphete skeleton. Variation

of the substitution pattern of 1,2-dihydrophosphete derivatives and chemical modification of their P atoms afford thermally stable derivatives which are suitable emitters to construct organic light-emitting diodes. The optical and the electrochemical properties of these new P-based

oligomers have been investigated in detail and are supported by DFT calculations. The OLED devices exhibit good performance and current independent CIE coordinates.

Keywords: Phosphorus, 1,2-dihydrophosphete, π -systems, OLED

Introduction

Organic light-emitting diodes (OLEDs) are key devices in the development of flat and flexible organic electronics. They have already been commercialized as components for displays and they have the potential for other promising applications such as solid state lighting.^[1] Despite the great success achieved by some commercial products in this area, the discovery and molecular engineering of novel electroluminescent emitting materials with improved electrical and optical properties are still relevant. With this aim, various heterocyclopentadienes (thiophene, silole...) have been

the reactive phosphorus center allow a tuning of the HOMO and LUMO levels, an improvement of the thermal stability, and a control of the solid state organisation of the π -systems, providing a simple and direct method for diversifying the structure and properties. This unique way of π -system molecular engineering afforded efficient materials for OLEDs, including white-emitting devices.^[3] These results prompted us to prepare and study the physical properties of other phosphacycles as building blocks for electroluminescent π -conjugated materials. Phosphorus heterocyclic chemistry is nowadays well-developed and many types of π -derivatives (4-,5-,6-,7-membered rings; presence of several heteroatoms...) are easily available on gram-scale.^[4] Among this diversity of structures, we focussed on the 1,2-dihydrophosphete skeleton for the development of π -conjugated materials for several reasons. This unsaturated building block has been known since the 80's, and its synthesis and reactivity have been widely investigated making this type of heterocycle easily accessible and well-understood.^[5] Within this family of P rings, 2-(diphenylmethylene)-1,4-diphenyl-1,2-dihydrophosphete skeleton (molecule **2a-f**, Scheme 1) appeared to us as an original platform for the development of novel P-materials for optoelectronic applications. Firstly, it possesses a π -conjugated system interacting with a phosphorus atom within a four-membered unsaturated ring. It was thus of interest to investigate the impact of P-modifications for tuning the electronic properties of this π -system. Note that the optical and electrochemical properties of this family of P-heterocycles have never been investigated. Secondly, the pyramidal shape of the P-atom affords steric hindrance which is a key parameter for solid-state engineering of chromophores since it should prevent the aggregation phenomena from taking place. Lastly, straightforward synthesis of phosphetes allowing easy derivatization are known and these rings appear to exhibit quite high chemical and thermal stability.

In this paper, we report on the synthesis of a new family of 1,2-dihydrophosphete derivatives **3a-f**, **4a**, **5a** (Scheme 1) and elucidation of their photophysical, thermal and electrochemical properties by following UV-Vis, photoluminescence, cyclovoltammetry, thermogravimetric analysis (TGA) and differential scanning calorimetry (DSC) studies. The use of these P-

[a] Prof. M. Hissler, Prof. R. Réau, Dr P.-A. Bouit, S. Pascal, Institut des Sciences Chimiques de Rennes, UMR6226 CNRS-Université de Rennes 1, Campus de Beaulieu, 35042 Rennes Cedex, France
E-mail: mhissler@univ-rennes1.fr, regis.reau@uni-rennes1.fr

[b] Prof. Z. Duan, Prof. F. Mathey, H. Chen, Z.Y. Wang, Z.S. Wang, Y.L. Zhang, College of Chemistry and Molecular Engineering, International Phosphorus Laboratory, Joint Research Laboratory for Functional Organophosphorus Materials of Henan Province, Zhengzhou University, Zhengzhou 450001, P. R. China
E-mail: duanzheng@zzu.edu.cn; fmathey@ntu.edu.sg

Prof. F. Mathey
Nanyang Technological University, CBC-SPMS, 21 Nanyang Link, Singapore 637371
E-mail: fmathey@ntu.edu.sg

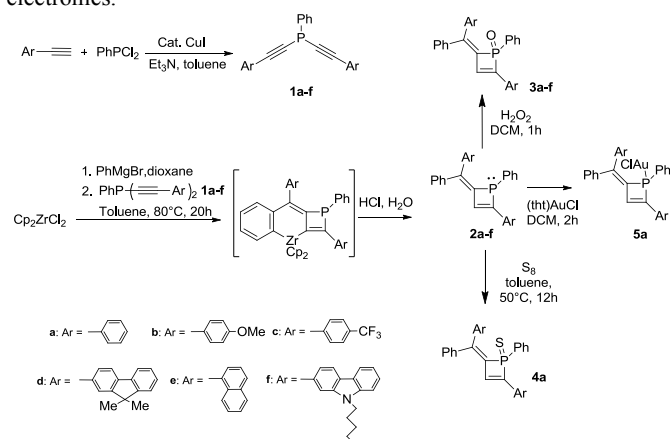
[c] B. Geffroy
Laboratoire de Chimie des Surfaces et Interfaces, CEA Saclay, IRAMIS, SPCSI, 91191 Gif-sur-Yvette, Cedex, France

[d] D. Tondelier
Laboratoire de Physique des Interfaces et Couches Minces, CNRS UMR 7647, Ecole Polytechnique, 91128 Palaiseau, France

Supporting information for this article is available on the WWW under <http://www.chemurj.org/> or from the author.

incorporated into the backbone of π -conjugated systems since their electronic properties are dependent on the nature of the heteroatom. For example, phospholes have received particular attentions as building blocks for the tailoring of functional π -conjugated systems for optoelectronic applications.^[2] One appealing property of this five-membered heterocycle is that simple chemical modifications of

rings as emitting materials in OLED devices is reported. These devices emit in the blue-green region, illustrating the potential of this novel P-platform for the development of materials for molecular electronics.



Scheme 1. Synthesis of the 1,2-dihydrophosphete derivatives

Results and Discussion

1,2-Dihydrophosphete derivatives **2a-f** were synthesized according to a straightforward one pot - four step procedure, devised by Majoral *et al.*^[5^e] (Scheme 1), involving an intramolecular coupling reaction of a dialkynylphosphane and zirconocene-benzene (Scheme 1). The starting materials **1a-f** (³¹P NMR: $\delta = ca. -60$ ppm) were obtained in medium to good yields (47-83%) via copper-catalyzed cross-coupling of terminal alkynes with dichlorophenylphosphine (Scheme 1).^[6] The presence of the Ph-substituents on the P-atom is essential for providing good solubility and stability to these derivatives. They were reacted with the transient benzyne complex, generated *in situ* by thermolysis of a solution of [Cp₂ZrPh₂] in toluene at 80°C, resulting in the formation of the corresponding benzo-zirconacyclohexadiene-phosphabutenes which upon treatment in acidic media gave access to the expected 1,2-dihydrophosphetes **2a-f** (³¹P NMR: $\delta = ca. +22.0$ ppm) (Scheme 1).^[5^{e-g}] Since the trivalent P-atom of 1,2-dihydrophosphetes is sensitive to oxidation, they were readily transformed into the σ^4 -derivatives **3a-f**, **4a** and **5a** by treatment with hydrogen peroxide, elemental sulfur and (tetrahydrothiophene)AuCl, respectively (Scheme 1).^[2] These compounds were purified by column chromatography and isolated as air-stable powders in good yields (34%-58%). The newly prepared P-compounds **1b-f**, **3a-f**, **4a** and **5a** were characterized by high-resolution mass spectrometry, elemental analysis, and their multinuclear NMR spectroscopic data support the proposed structures. It is noteworthy that this synthetic route is rather simple and efficient, allowing both gram-scale preparation and introduction of a large variety of functional groups (electron-withdrawing and electron-donating substituents) on the organophosphorus backbone through functionalization of the starting dialkynylphosphanes **1** (Scheme 1). Furthermore, P-functionalization allows additional straightforward derivatization (P=O, P=S, P-AuCl) of these π -conjugated platforms.

The structure of the gold complex **5a** was investigated by X-ray crystallography in order to gain insight into the organization of the phosphete derivatives in the solid state (Figure 1). Single crystals of **5a** suitable for X-ray diffraction study were grown upon diffusion of pentane into a dichloromethane solution. The metric data of the phosphete-AuCl subunit are classical (Table 1).^[3e] For

example, the phosphorus center adopts a distorted tetrahedral geometry ($\sum P_{ang} = 294.8^\circ$) and the endocyclic P-C bond lengths [1.830 (6) Å, Table 1] approach that of a P-C single bond (1.84 Å). The geometry around Au atom is almost linear (P-Au-Cl, 178.69 (6)°). The π -conjugated backbone including the dihydrophosphete ring and the substituents in position 2 and 4 (exocyclic double bond and phenyl ring) are planar (maximum deviation from the mean C-*sp*² plane, 0.06 Å) and the C-C bond lengths ($d_{C3-C4} = 1.455$ (8) Å, $d_{C1-C2} = 1.462$ (9) Å, Figure 1) between the double bonds are in the range expected for (C(*sp*²)-C(*sp*²)) single bonds. These data indicate the presence of an extended π conjugation including the endocyclic double bond of the phosphete and the substituents in the 2- and 4-positions (exocyclic double bond and phenyl ring). Note that the two lateral phenyl substituents of the C10 atom (Figure 1) are twisted with respect to this main C-*sp*² plane (twist angles, 44.2° and 59.2°) due to H-H repulsion.

The solid-state organization of complex **5a** (Figure 1) shows no intermolecular π - π , CH- π or auriphilic ($d(Au-Au) > 5.3$ Å) interactions. This property is likely due to the presence of out-of-Cp²-planes substituents (P- and C10-substituents) which provide steric hindrance. This property is promising in the prospect of using these compounds as emitters in OLEDs since aggregation of emitting materials is known to reduce the efficiency of these devices.

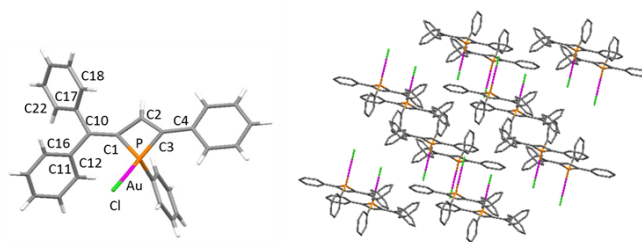


Figure 1. Structure and packing of the gold complex **5a** in the solid state

Table 1 Selected bond lengths [Å] and twist angles between the phosphete ring and its 2- and 4-Substituents [°] for the gold complex **5a**.

Bond length		Angles	
P-(C1)	1.830(6)	(C1)-P-(C3)	74.5(3)
(C1)-C2)	1.462(9)	(C1)-P-(C23)	115.2(2)
(C2)-(C3)	1.363(8)	C(1)-P-Au	119.4(2)
(C3)-P	1.829(6)	(C3)-P-(C23)	107.3(3)
P-Au	2.2237(19)	C(3)-P-Au	120.9(2)
Au-Cl	2.291(2)	C(23)-P-Au	115.2(2)
(C1)-(C10)	1.349(8)	P-Au-Cl	178.69(7)
(C3)-(C4)	1.455(8)		

In order to establish the structure-property relationship for this novel series of P-based π -conjugated systems (Scheme 1), their UV-vis absorption, excitation and fluorescence spectra were measured in CH₂Cl₂ (Table 2). It is noteworthy that the polarity and the hydrogen-bond donor ability (HDBA) of the solvent have a negligible effect on the absorption and emission properties and the UV-vis absorption maxima are in very good agreement with the excitation data (see SI, Figure S1-4).

Table 2. Photophysical, electrochemical and thermal data for **3a-f**, **4a**, **5a**.

	λ_{max} [nm] ^[a]	ϵ [M ⁻¹ .cm ⁻¹]	λ_{em} [nm] ^[a]	Φ_f (%) ^[b]	T _{TGA} [°C] ^[c]	T _m [°C] ^[d]	E _{ox} ¹ [V] ^[e]	E _{red} ¹ [V] ^[e]
3a	358	36900	426	2.4	316	205	-	-2.19

3b	375	36800	445	1.6	320	75	+0.76 ^[b]	- ^[f]
3c	360	30100	426	0.6	300	165	- ^[f]	-1.87 ^[b]
3d	400	50000	458/480	6.6	375	230	+0.79 ^[b]	-2.09 ^[b]
3e	375	33200	456	5.2	340	- ^[f]	+1.19	-2.14
3f	409	36200	483	12.4	345	- ^[f]	+0.49 ^[b]	-2.46
4a	358	27700	421	0.5	330	152	+1.03	-2.13 ^[h]
5a	359	33200	425	0.9	300	130	+1.15	-2.09

[a] Measured in CH₂Cl₂ (5.10⁻⁵M). [b] Measured relative to quinine sulfate (H₂SO₄, 0.1 M), ± 15%. [c] Onset weight-loss temperature estimated using TGA under nitrogen. [d] Melting point measured by DSC under Argon, 10°C/min. [e] All potentials were obtained during cyclic voltammetric investigations in 0.2 M Bu₄NPF₆ in CH₂Cl₂. Platinum electrode diameter 1 mm, sweep rate: 200 mV s⁻¹. All potentials are referenced to the reversible formal potential of ferrocene/ferrocenium. [f] not observed [h] reversible process.

Compounds **3-5a** display an intense band in the UV-visible region centered at 358 nm, attributed to π - π^* transitions of the extended π -conjugated system including the dihydrophosphete ring and substituents in position 2 and 4 (exocyclic double bond and phenyl ring). Interestingly, these derivatives exhibit blue emissions (Figure 2) albeit with low quantum yields ($\Phi_f = 0.5$ -2%, Table 2). The presence of the “bridging phosphorus atom” impacts the optical properties compared to the 1,1,4-triphenylbutadiene.^[7] Due to a partial rigidification of the π -system, red-shifted structured absorption and emission bands are observed for the dihydrophosphete compound, suggesting a better electron delocalization along the π -system and a small rearrangement of these molecules upon photoexcitation. In return, the substituent on the P-atom has a very weak impact on the optical transitions but clearly impacts the quantum yield, with best performance for the P=O derivative **3a** (Table 2). Interestingly, the introduction of electron-rich substituents (**3b**) induces a bathochromic shift of absorption and emission maxima while the introduction of electron deficient substituents (**3c**) has no impact on the optical properties. This effect is attributed to an intramolecular charge transfer from the electron-donating group to the electron-deficient dihydro-oxophosphete center. Moreover, upon extension of the π -conjugated system, all optical features are significantly red-shifted from those of compound **3a** (Table 2). The smallest bathochromic shift is observed with the naphthalene substituted oligomer **3e** ($\lambda_{\text{abs}} = 375$ nm, $\lambda_{\text{em}} = 456$ nm). The fluorene and the carbazole substituted oligomers (**3d**, **3f**) show significantly red-shifted maxima of absorption and emission (**3d**, $\lambda_{\text{abs}} = 400$ nm, $\lambda_{\text{em}} = 468$ nm; **3f**, $\lambda_{\text{abs}} = 409$ nm, $\lambda_{\text{em}} = 483$ nm) indicating an increased effective conjugation length in both molecules compared to the compound **3a**. Furthermore, Compounds **3d-f** display an emission band in the 460-480 nm range with moderate quantum yield in solution (5 % < Φ_f < 12 %) making them a good candidate to act as blue emitter in OLED devices.

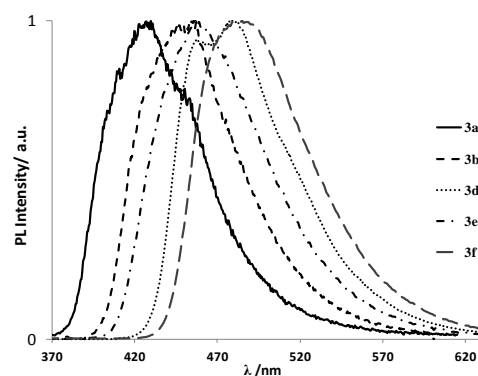


Figure 2. Normalized emission spectra of **3a**, **b**, **d**, **e**, **f** recorded in dichloromethane (5.10⁻⁶ M).

In order to gain a deeper understanding of the electronic structure of these phosphete derivatives (Figure 3), DFT calculations at the B3LYP/6-31+G(d, p) level were carried out to obtain orbital distributions of the highest occupied molecular orbitals (HOMO, HOMO-1) and the lowest unoccupied molecular orbital (LUMO) energy levels. As shown in Figure 3, the calculated optimized structure of derivative **2a** shows that the π -conjugated backbone, including the dihydrophosphete ring and substituents in position 2 and 4 (exocyclic double bond and phenyl ring), is planar and is similar to the structure of **5a** (Figure 1). The HOMO and the LUMO energy levels are localized on the entire π -conjugated carbon framework and the contribution of the phosphorus lone pair is mainly localized in the HOMO-1. Since the difference in energy between the HOMO-1 and HOMO is significant and neither the HOMO nor the LUMO show a sizeable localization at phosphorus, the chemical modifications on the phosphorus atom will have negligible impact on the HOMO-LUMO gap, as observed by UV-vis absorption.

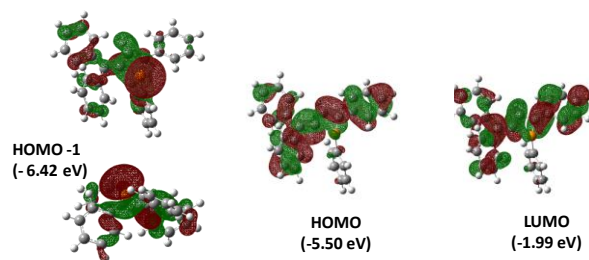


Figure 3. Calculated molecular orbital amplitude plots of HOMO -1, HOMO and LUMO levels of **2a**.

The impact of these chemical modifications performed on the P-atom (**3a**) or on the π -system by introduction of electron rich or deficient substituents (**3b** and **3c** respectively) on the molecular orbital levels has also been rationalized by DFT calculations. As observed for **2a** (*vide supra*), the computed molecular orbitals of **3a-c** are fully delocalized over the entire backbone. The oxidation of P-atom induces a stabilization of the molecular orbital levels as well as a reduction of the HOMO-LUMO gap (see Figure S5 and Figure 3). The introduction of electron-rich substituents on the π -system induces a reduction of the HOMO-LUMO gap by a pronounced increase of the HOMO energy level of **3b** while the introduction of electron withdrawing group (**3c**) stabilizes in a similar manner the HOMO and the LUMO level inducing no reduction of the HOMO-

Table 3. EL performance of devices as function of the device structure and the doping rate

Device ^[a]	EML ^[b]	$\lambda_{\max}^{\text{EL}}$	External quantum efficiency	Current efficiency ^[c]	Power efficiency ^[c]	CIE coordinates
		[nm]				
	Doping rate [wt. %]		[%]	[cd A ⁻¹]	[lm W ⁻¹]	(x,y)
A	3d	468/505	0.9	2.2	0.6	(0.27, 0.46)
B	CBP: 3d (2.5%)	492	0.7	1.3	0.4	(0.17, 0.32)
C	DPVBi: 3d (2.5%)	492	2.5	5.1	1.4	(0.18, 0.34)
D	CBP: 3e (2.7%)	476	0.4	0.6	0.2	(0.16, 0.24)
E	DPVBi: 3e (1.3%)	474	1.6	2.8	0.8	(0.17, 0.27)
F	DPVBi: 3e (2.3%)	480	1.4	2.6	0.7	(0.18, 0.29)
G	DPVBi: 3e (7.2%)	484	1.1	2.3	0.7	(0.20, 0.32)
H	DPVBi: 3f (1.6%)	488	1.2	2.3	0.6	(0.18, 0.31)
I	DPVBi: 3f (4.0%)	500	1.1	2.4	0.7	(0.20, 0.39)
ref	DPVBi	468	2.1	3.2	0.9	(0.16, 0.22)

[a] Device configuration (thickness): ITO/CuPc (10 nm)/ α -NPB (50 nm)/ EML (15 nm)/ DPVBi (35 nm)/BCP (10 nm)/Alq₃ (50 nm)/LiF (1.2 nm)/Al (100 nm); [b] EML (Emitting Layer) = P-emitter, DPVBi or CBP as host [c] Measured at 20 mA/cm².

LUMO gap (see Figure S5). All these assumptions are nicely supported by the optical and the electrochemical data.

Cyclic voltammetry (CV), recorded in CH₂Cl₂ using Bu₄NPF₆ as electrolyte, was used to investigate the redox properties of **3a-f**, **4a** and **5a** (Table 2). Compounds **3-5a** display different electrochemical behaviours depending on the P-substitution. Compound **3a** presents only an irreversible electronic reduction wave ($E_{\text{red1}}^{\circ} = -2.19$ V vs. Fc^{+/0}) in the electrochemical window. While replacing O by S in **4a**, an irreversible electronic oxidation wave is observed ($E_{\text{ox1}}^{\circ} = +1.03$ V vs. Fc^{+/0}) and the reduction becomes reversible ($E_{\text{red1}}^{\circ} = -2.13$ V vs. Fc^{+/0}). Coordination to Au(I) slightly modifies the potentials (see Table 3) while keeping the electrochemical gap constant (around 3.0 eV). All these observations demonstrate that chemical modifications performed at the P-atom impact weakly the HOMO and LUMO's energy of the phosphite compounds. As anticipated, introduction of electron-donating groups cathodically shifts the oxidation wave ($E_{\text{ox1}}^{\circ} = +0.76$ V vs. Fc^{+/0} for **3b**) while the introduction of electron withdrawing group anodically shifts the reduction wave ($E_{\text{red1}}^{\circ} = -1.87$ V vs. Fc^{+/0} for **3c**). Furthermore, the introduction of emissive subunits like fluorene (**3d**), naphthalene (**3e**) or carbazole (**3f**) also affects the redox potential. For example, compound **3d** displays amphoteric redox character with quasi-reversible electrochemical waves (see Table 2) making it appealing for application in optoelectronic devices. This study clearly shows that modifications of both π -conjugated system and P-environment impact the electrochemical properties of the compounds and allow fine tuning of its bandgap.

Interestingly, dihydrophosphite derivatives **3a-f**, **4a** and **5a** display excellent thermal stability (Table 2). Thermogravimetric analyses (TGA) measurements performed under nitrogen atmosphere show that the whole family of compounds display decomposition temperatures above 300°C, which allows them to be used in "small molecule" OLEDs technology. Particularly, fluorene-substituted compound **3d** shows a decomposition temperature at 10% weight loss (T_{d10}) of 375 °C. Differential scanning calorimetry (DSC) measurements show that their melting points (T_m) were in the range of 75-230°C (Table 2). The formation of a glassy state of these derivatives after melting and cooling was evidenced (for example, T_g (**3d**): 127 °C). Further heating above the glass transition temperature and cooling down to 25°C resulted in no further

crystallization or melting behaviors. These results indicate that they present good morphological and thermal stabilities, two critical issues for operating stability and lifetime of the devices.

Since the derivatives **3d-f** (Scheme 1) are thermally stable and emissive (Table 2), they can be used as emitters in multilayer OLEDs. First, compound **3d** was used as a pure emitting layer (EML) in multilayer OLED **A** (Table 3) having an indium tin oxide (ITO)/ copper phthalocyanine (CuPc) (10 nm) / N,N'-diphenyl-N,N'-bis(1-naphthylphenyl)-1,1'-biphenyl-4,4'-diamine (α -NPB) (50 nm) / EML (15 nm) / 4,4'-bis(2,2'-diphenylvinyl)biphenyl (DPVBi) (35 nm) / bathocuproine (BCP) (10 nm) / tris(8-hydroxyquinolinato)aluminium (Alq₃) (50 nm) / LiF (1.2 nm) / Al (100 nm) configuration (see Figure S6). The electroluminescence (EL) spectrum of device **A** ($\lambda_{\text{maxEL}} = 500$ nm) resembles the thin film PL spectrum of derivative **3d** ($\lambda_{\text{em}} = 502$ nm) showing that the EL emission bands are from this P-luminophore. Furthermore the increase of the current density does not impact the emission wavelength of device **A** (Figure 4), proving that this emission is not due to degradation of the material. The luminance of this device reaches 1000 cd.m⁻² at 20 mA.cm⁻² with current and power efficiencies of 2.19 cd.A⁻¹ and 0.61 lm.W⁻¹, respectively (Table 3). These moderate performances have been assigned to the moderate charge carrier conduction properties of the EML. In order to improve the device performance, we incorporated the P-fluorophore **3d** in two matrices having similar HOMO and LUMO energy levels but different charge transport properties: 4,4'-bis(2,2'-diphenylvinyl)biphenyl (DPVBi) and 4,4'-N,N'-dicarbazole-biphenyl (CBP). CBP possesses a hole mobility at least one order of magnitude higher than its electron mobility^[8] and DPVBi is usually used as blue emitter matrix and electron transporting layer (ETL) in OLEDs.^[9] For a doping rate (DR) of 2.5%, the EL spectrum of the devices **B** (CBP matrix) and **C** (DPVBi matrix) exhibit only the characteristic emission of the P-derivative **3d**, no emission of the matrix is observed but the performance of these diodes is affected by the nature of the host material (Table 3). The device **C** using DPVBi as host exhibits much higher efficiencies compared to the device **B** using CBP matrix. Effectively, the external quantum efficiency, current and power efficiencies have been multiplied by ≈ 4 . This effect can be explained by a better charge transport as shown in Figure 5 where the J-V curve for the device **C** comprising DPVBi as host is shifted to lower voltages comparatively to device **B** (CBP

matrix). Furthermore the performance of device **C** is very satisfying with a brightness of 3000 cd.m⁻² at 20 mA/cm² (Figure S9). Moreover, the brightness regularly increases with the current density (see SI) showing the good stability of this OLED. Similar observation has been made with P-fluorophore **3e** (Table 3, Figure S10-11), only the EL emission maximum has been blue-shifted ($\lambda_{em} = 474$ nm, Table 3) compared to device **C** due to the presence of the naphthalene substituents. Since the device with DPVBi host had the best performance, we decided to keep the DPVBi matrix for studying the effect of the doping ratio on the EL performance when compounds **3e** and **3f** were used as emitters. As it can be seen in Table 3 (devices **E**, **F**, **G**, **H** and **I**) the performance of the devices is not changed by an increase of the doping ratio. Even for high doping ratio (device **G**) the quenching effect is limited due to the particular property of the P-molecules avoiding the formation of strong aggregates^[3b]. The increase of the doping rate induces only a small variation of the EL emission wavelength and on the CIE coordinates.

In summary, all the P-fluorophores present a greenish-blue emission. The best performance has been obtained for **3d** used as dopant in a DPVBi host (device **C**) with a current efficiency up to 5.1 cd/A, which is fairly good for a fluorescent blue emitter. It is worthy to note that this value is higher than for the reference blue device with DPVBi as emitter (device **ref**, Table 3).

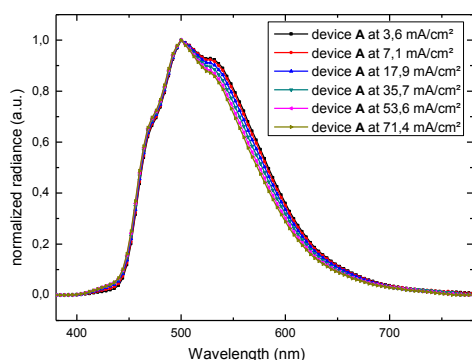


Figure 4. EL emission spectra of the diode **A** at different current densities.

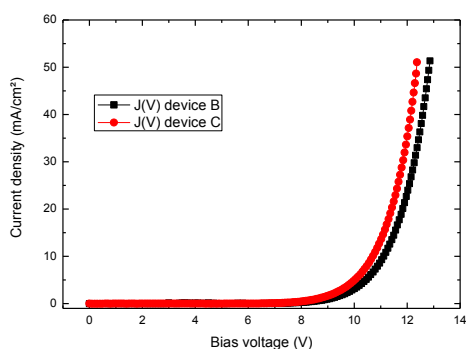


Figure 5. J-V characteristics of devices **B** and **C**

Conclusion

In conclusion, the 1,2-dihydrophosphate skeleton is an interesting building block for the development of new π -conjugated oligomers. Variation of the substitution pattern of 1,2-dihydrophosphate derivatives and chemical modification of their P atoms afford thermally stable derivatives which are suitable emitters to construct efficient organic light emitting diodes. For example, OLEDs

containing the phosphite-based compound **3d** as emitter exhibit blue electroluminescence, good performances and current independent CIE coordinates.

Experimental Section

General Procedures. All experiments were performed under an atmosphere of dry nitrogen using standard Schlenk techniques. Column chromatography was performed in air, unless stated in text. Solvents were freshly distilled under nitrogen from sodium/benzophenone (tetrahydrofuran, diethylether) or from phosphorus pentoxide (dichloromethane, toluene). All reagents were used as received and used directly without further purification. Silica gel (200-300 mesh) for purification and silica gel TLC (F254) were purchased from Qing Dao Hai Yang Chemical Industry Co. of China. ¹H, ¹³C, and ³¹P NMR spectra were recorded on a Bruker DPX-300 or AVANCE III-400 Spectrometer. ¹H and ¹³C NMR chemical shifts were reported in parts per million (ppm) relative to Si(CH₃)₄ as external standard. ³¹P NMR downfield chemical shifts were expressed with a positive sign, in ppm, relative to external 85 % H₃PO₄. High-resolution mass spectra were obtained on a Varian MAT 311, Waters Q-TOF 2 or ZabSpec TOF Micromass instrument at CRMPO, University of Rennes 1. Elemental analyses were performed by the CRMPO, University of Rennes 1.

Determination of optical data: UV/Vis spectra were recorded at room temperature on a Varian Cary 5000 UV-Vis-NIR spectrophotometer. Luminescence spectra were recorded at room temperature with a FS920 Steady State Fluorimeter (M300, UC920, CD920/CD930, S900) using a xenon lamp (Xe900). All spectra were recorded in CH₂Cl₂ (SDS, HPLC grade) stabilized with ethanol, with concentrations of 5.10⁻⁶, 10⁻⁵, 5.10⁻⁵ and 10⁻⁴ M. Quantum yields were calculated relative to quinine sulfate ($\Phi = 0.546$ in H₂SO₄ 0.1N)^[10], using the following equation $Q_x/Q_r = [A_r(\lambda)/A_x(\lambda)][n_x^2/n_r^2][D_x/D_r]$ where A is the absorbance at the excitation wavelength (λ), n the refractive index and D the integrated luminescence intensity. "r" and "x" stand for reference and sample. Excitations of references and samples compounds were performed at the maximum wavelength of the molecules.

Cyclic voltammetry measurements: The electrochemical studies were carried out under argon using an Eco Chemie Autolab PGSTAT 30 potentiostat for cyclic voltammetry with the three-electrode configuration: the working electrode was a platinum disk, the reference electrode a saturated calomel electrode and the counter-electrode a platinum wire. All potential were internally referenced to the ferrocene/ferrocenium couple. For the measurements concentrations of 10⁻³ M of the electroactive species were used in freshly distilled and degassed dichloromethane (*Lichrosolv*, Merck) and 0.2 M tetrabutylammonium hexafluorophosphate (TBAHFP, Fluka) which was twice recrystallized from ethanol and dried under vacuum prior to use.

Device fabrication and characterization: EL devices, based on a multilayer structure have been fabricated onto patterned ITO coated glass substrates from XinYan Technology (thickness: 100 nm and sheet resistance: less of 20 Ω /m). The organic materials (from Aldrich and Lumtec) are deposited onto the ITO anode by sublimation under high vacuum (< 10⁻⁶ Torr) at a rate of 0.2 – 0.3 nm/s. The common structure of all the devices is the following: a thin layer (10 nm thick) of copper phthalocyanine (CuPc) is used as hole injection layer (HIL) and 50 nm of N,N'-diphenyl-N,N'-bis(1-naphthylphenyl)-1,1'-biphenyl-4,4'-diamine (α -NPB) as hole transporting layer (HTL). The emitting layer consists of 15 nm thick film of pure phosphite derivatives or DPVBi (or CBP) doped phosphite derivatives. The doped layer is obtained by co-evaporation of the two compounds and the doping rate is controlled by tuning the evaporation rate of each material. A thin layer of bathocuproine (BCP) (10 nm) is used as hole blocking layer. Alq₃ (10 nm) is used as electron transporting layer (ETL). Finally, a cathode consisting of 1.2 nm of LiF capped with 100 nm of Al is deposited onto the organic stack. The entire device is fabricated in the same run without breaking the vacuum. In this study, the thicknesses of the different organic layers were kept constant for all the

devices. The active area of the devices defined by the overlap of the ITO anode and the metallic cathode was 0.28 cm².

The current-voltage-luminance (I-V-L) characteristics of the devices were measured with a regulated power supply (Laboratory Power Supply EA-PS 3032-10B) combined with a multimeter and a 1 cm² area silicon calibrated photodiode (Hamamatsu). The spectral emission was recorded with a SpectraScan PR655 spectrophotometer. All the measurements were performed at room temperature and at ambient atmosphere with no further encapsulation of devices immediately after the device realization.

Details of the X-ray crystallography study: single crystal data collection were performed at 100 K with an APEX II Bruker-AXS (Centre de Diffraction, Université de Rennes 1, France) with Mo-K α radiation ($\lambda = 0.71073$ Å). Reflections were indexed, Lorentz-polarization corrected and integrated by the DENZO program of the KappaCCD software package. The data merging process was performed using the SCALEPACK program.^[11] Structure determinations were performed by direct methods with the solving program SIR97^[12] that revealed all the non hydrogen atoms. SHELXL program (G.M. Sheldrick SHELX97, Program for the Refinement of Crystal Structures, University of Göttingen, Germany, 1997) was used to refine the structures by full-matrix least-squares based on F^2 . All non-hydrogen atoms were refined with anisotropic displacement parameters. Hydrogen atoms were included in idealized positions and refined with isotropic displacement parameters. Atomic scattering factors for all atoms were taken from International Tables for X-ray Crystallography.^[13] Details of crystal data and structural refinements are given in Table S2.

Crystallographic data. CCDC-948792 reference number contains the supplementary crystallographic data for **5a** respectively. These data can be obtained free of charge at www.ccdc.cam.ac.uk/conts/retreving.html or from the Cambridge Crystallographic Data Center, 12 union Road, Cambridge CB2 1EZ, UK; Fax: (internat.) + 44-1223-336-033; E-mail: deposit@ccdc.cam.ac.uk.

Calculations on the phosphite derivatives: All the density functional calculations were carried out using the Gaussian 03 code. This level of the theory has provided satisfactory results for the phosphite oligomers.^[14] The geometries were fully optimized, and vibrational analysis was performed on the optimized structures to check whether the stationary point located is a minimum of the potential energy hypersurface. The density functional theory (DFT) calculation and structure optimization of **2a**, **3a-c** were conducted at the B3LYP/6-31+G (d, p) level.

Experimental part

a) Synthesis of **1a-f**.

Phenylbis(2-phenylethynyl)phosphine (**1a**) was prepared according to the previously reported procedure^[15]. A similar procedure was used to prepare **1b-f**. The typical procedure is as follows: a mixture of terminal alkyne (12.8 mmol), PhPCl₂ (0.7 mL, 5.2 mmol), CuI (0.1 g, 0.52 mmol), NEt₃ (4.35 mL) and toluene (35 mL) was stirred at room temperature for 12 h. After filtration and removal of the solvent, the residue was chromatographed over silica gel (hexane) to give **1**.

*Synthesis of **1b**:* The compound **1b** is obtained as yellow solid (1.60 g, 4.3 mmol, Yield: 83 %). ³¹P NMR (CDCl₃; 121 MHz): $\delta = -60.7$ (s). ¹H NMR (CDCl₃; 300 MHz): $\delta = 3.82$ (s, 6H, OCH₃), 7.18 (AB system, 8H, $J_{AB} = 8.9$ Hz, $\Delta\nu_{AB} = 188.3$ Hz, CH_{phenyl}-OCH₃), 7.44-7.51 (m, 3H, CHphenyl), 7.87-7.93 (m, 2H, CHphenyl); ¹³C NMR (CDCl₃; 75 MHz): $\delta = 55.3$ (s, OCH₃), 81.4 (s, C \equiv C), 106.5 (d, $J(C,P) = 7.4$ Hz, C \equiv C), 113.9 (s, CHphenyl), 114.6 (s, Cphenyl), 128.8 (d, $J(C,P) = 7.6$ Hz, CHphenyl), 129.3 (s, CHphenyl), 132.0 (d, $J(C,P) = 21.8$ Hz, CHphenyl), 133.7 (d, $J(C,P) = 1.5$ Hz, CHphenyl), 133.8 (s, Cphenyl), 160.3 (s, Cphenyl). MS (ESI, MeOH, m/z): [M+K]⁺ calcd for C₂₄H₁₉O₂KP, 409.07; found 409.1.

*Synthesis of **1c**:* The compound **1c** is obtained as brown solid (1.09 g, 2.4 mmol, Yield: 47 %). ³¹P NMR (CDCl₃; 121 MHz): $\delta = -61.6$ (s). ¹H NMR (CDCl₃; 300 MHz): $\delta = 7.47$ -7.50 (m, 3H, CHphenyl), 7.59-7.65 (m, 8H, CHphenyl), 7.86-7.92 (m, 2H,

CHphenyl); ¹³C NMR (CDCl₃; 75 MHz): $\delta = 85.5$ (d, $J(C,P) = 6.3$ Hz, C \equiv C), 104.8 (d, $J(C,P) = 6.4$ Hz, C \equiv C), 123.8 (q, $J(C,F) = 270.6$ Hz, CF₃), 125.3 (q, $J(C,F) = 3.7$ Hz, CHphenyl), 126.0 (s, Cphenyl), 129.1 (d, $J(C,P) = 8.2$ Hz, CHphenyl), 130.1 (s, CHphenyl), 130.8 (q, $J(C,F) = 32.6$ Hz, Cphenyl), 132.0 (s, Cphenyl), 132.17 (d, $J(C,P) = 1.6$ Hz, CHphenyl), 132.5 (d, $J(C,P) = 22.4$ Hz, CHphenyl). MS (ESI, MeOH, m/z): [M+K]⁺ calcd for C₂₄H₁₃F₆KP, 485.03; found 485.0.

*Synthesis of **1d**:* The compound **1c** is obtained as white solid (1.38 g, 2.5 mmol, Yield: 49 %). ³¹P NMR (CDCl₃; 121 MHz): $\delta = -60.7$ (s). ¹H NMR (CDCl₃; 300 MHz): $\delta = 1.65$ (s, 12H, CH₃), 7.50-7.90 (m, 17H, CHphenyl), 8.32 (t, 2H, $J(H,H) = 8.4$ Hz, $J(H,P) = 8.4$ Hz, CHphenyl). ¹³C NMR (CDCl₃; 75 MHz): $\delta = 27.2$ (s, CH₃), 47.1 (s, C(CH₃)₂), 83.3 (s, C \equiv C), 107.8 (d, $J(C,P) = 7.4$ Hz, C \equiv C), 120.3 (s, CHphenyl), 120.8 (s, CHphenyl), 121.1 (s, Cphenyl), 123.0 (s, CHphenyl), 126.7 (s, CHphenyl), 127.5 (s, CHphenyl), 128.3 (s, CHphenyl), 129.3 (d, $J(C,P) = 7.8$ Hz, CHphenyl), 129.9 (s, CHphenyl), 131.7 (s, CHphenyl), 132.6 (d, $J(C,P) = 21.8$ Hz, CHphenyl), 133.8 (s, Cphenyl), 138.5 (s, Cphenyl), 140.6 (s, Cphenyl), 153.8 (s, Cphenyl), 154.2 (s, Cphenyl). MS (ESI, MeOH, m/z): [M+H]⁺ calcd for C₄₀H₃₂P, 543.2; found 543.2.

*Synthesis of **1e**:* The compound **1e** is obtained as white solid (1.77 g, 4.3 mmol, Yield: 83 %). ³¹P NMR (CDCl₃; 121 MHz): $\delta = -60.8$ (s). ¹H NMR (CDCl₃; 300 MHz): $\delta = 7.49$ -7.68 (m, 9H, CHaromatic), 7.89-7.94 (m, 6H, CHaromatic), 8.22 (t, 2H, $J(H,H) = 8.4$ Hz, $J(H,P) = 9.0$ Hz, CHaromatic), 8.56 (d, 2H, $J(H,H) = 8.1$ Hz, CHaromatic). ¹³C NMR (CDCl₃; 75 MHz): $\delta = 88.3$ (d, $J(C,P) = 4.5$ Hz, C \equiv C), 104.8 (d, $J(C,P) = 6.8$ Hz, C \equiv C), 120.2 (s, Caromatic), 125.3 (s, CHaromatic), 126.2 (s, CHaromatic), 126.7 (s, CHaromatic), 127.3 (s, CHaromatic), 128.5 (s, CHaromatic), 129.2 (d, $J(C,P) = 8.0$ Hz, CHaromatic), 129.9 (s, CHaromatic), 131.3 (d, $J(C,P) = 1.7$ Hz, CHaromatic), 132.4 (s, CHaromatic), 132.7 (s, CHaromatic), 133.2 (s, Caromatic), 133.5 (s, Caromatic), 133.6 (s, Caromatic). MS (ESI, MeOH, m/z): [M+H]⁺ calcd for C₃₀H₂₀P, 411.5; found 411.3.

*Synthesis of **1f**:* The compound **1f** is obtained as white solid (2.02 g, 3.2 mmol, Yield: 62 %). ³¹P NMR (CDCl₃; 121 MHz): $\delta = -61.4$ (s). ¹H NMR (CDCl₃; 300 MHz): $\delta = 0.90$ (t, 6H, $J(H,H) = 6.9$ Hz, CH₃), 1.35-1.38 (m, 8H, CH₂), 1.85-1.89 (m, 4H, CH₂), 4.28 (t, 4H, $J(H,H) = 7.2$ Hz, N-CH₂), 7.26-7.55 (m, 11H, CHphenyl), 7.67 (dd, 2H, $J(H,H) = 1.2$ Hz, $J(H,H) = 8.4$ Hz, CHphenyl), 8.03-8.05 (m, 2H, CHphenyl), 8.09 (d, 2H, $J(H,H) = 7.8$ Hz, CHphenyl), 8.34 (s, 2H, CHphenyl). ¹³C NMR (CDCl₃; 75 MHz): $\delta = 14.1$ (s, CH₃), 22.6 (s, CH₂), 28.8 (s, CH₂), 29.4 (s, CH₂), 43.2 (s, CH₂), 80.9 (s, C \equiv C), 108.3 (d, $J(C,P) = 7.7$ Hz, C \equiv C), 108.8 (s, CHphenyl), 109.1 (s, CHphenyl), 112.5 (s, Cphenyl), 119.6 (s, CHphenyl), 120.6 (s, CHphenyl), 122.5 (s, Cphenyl), 122.8 (s, Cphenyl), 124.9 (s, CHphenyl), 126.3 (s, CHphenyl), 128.9 (d, $J(C,P) = 7.5$ Hz, CHphenyl), 129.3 (s, CHphenyl), 129.8 (s, CHphenyl), 132.2 (d, $J(C,P) = 21.2$ Hz, CHphenyl), 134.6 (s, Cphenyl), 140.6 (s, Cphenyl), 140.8 (s, Cphenyl). MS (ESI, MeOH, m/z): [M+H]⁺ calcd for C₄₄H₄₂N₂P, 629.8; found 629.6.

b) Synthesis of **2a-f**, **3a-f**, **4a** and **5a**.

*Synthesis of **3a**:* Bromobenzene (312 μ L, 3.0 mmol) was added to a distilled ether solution (20 mL) containing an excess of Mg (86 mg, 3.6 mmol) at room temperature. After 1 h of stirring at 40 °C, Cp₂ZrCl₂ (292 mg, 1.0 mmol) was introduced in the solution. The solution was stirred until complete dissolution of the solid, then dioxane (258 μ L, 3.0 mmol) was added generating a white precipitate. The mixture was stirred for 1 h at room temperature and the solvent was evaporated under vacuum. The white solid was dissolved in 20 mL of degassed toluene and Phenylbis(2-phenylethynyl)phosphine **1a** (293 mg, 0.95 mmol) was added. After 20h of stirring at 80°C, a solution of 20 mL toluene charged with HCl gas (from NH₄Cl + H₂SO₄) was added to the mixture at 0 °C. After 1 h of stirring at room temperature, the solution was filtered and the solvent was removed under vacuum. The crude residue was dissolved in 10 mL CH₂Cl₂ and an excess of H₂O₂ (5 mL) was added. After 1 h of stirring at room temperature, water was added (10 mL) to the reaction mixture and the aqueous layer was extracted with CH₂Cl₂ (3 x 5 mL). The organic layer was dried over anhydrous MgSO₄ and the solvent was evaporated under vacuum. The crude product was purified by chromatography on silica (Petroleum ether/AcOEt, 2/1, v/v). The recovered fraction

was crystallized in Et₂O to get a pure white solid in a 56% yield (215 mg, 0.53 mmol). ³¹P NMR (CDCl₃; 121 MHz): δ = +35.6 (s). ¹H NMR (CDCl₃; 300 MHz): δ = 7.23-7.63 (m, 18H, CHphenyl), 7.89 (d, 1H, J(H,P) = 70.5 Hz, =CH), 7.87 (dd, 2H, J(H,P) = 12.0 Hz, J(H,H) = 7.5 Hz, CHphenyl). ¹³C NMR (CDCl₃; 75 MHz): δ = 127.2 (d, J(C,P) = 8.9 Hz, CHphenyl), 128.3 (s, CHphenyl), 128.4 (s, CHphenyl), 128.5 (s, CHphenyl), 128.6 (s, CHphenyl), 128.9 (s, CHphenyl), 129.0 (d, J(C,P) = 11.9 Hz, CHphenyl), 129.1 (s, CHphenyl), 129.8 (s, CHphenyl), 129.9 (s, CHphenyl), 130.7 (d, J(C,P) = 85.1 Hz, Cipso), 131.0 (d, J(C,P) = 5.8 Hz, Cphenyl), 131.2 (d, J(C,P) = 11.3 Hz, CHphenyl), 132.5 (d, J(C,P) = 2.7 Hz, CHphenyl), 139.3 (d, J(C,P) = 8.8 Hz, Cphenyl), 139.4 (d, J(C,P) = 16.9 Hz, Csp₂), 140.0 (s, Cphenyl), 142.1 (d, J(C,P) = 77.0 Hz, Csp₂), 144.7 (d, J(C,P) = 12.5 Hz, =CH), 155.7 (d, J(C,P) = 78.4 Hz, Csp₂). HR-MS (ESI, CHCl₃/MeOH, 50/50, v/v, m/z): [M+Na]⁺ calcd for C₂₈H₂₁ONaP, 427.12277; found 427.1228; Anal. Calcd for C₂₈H₂₁OP (404.45): C 83.15, H 5.23, found: C 82.37, H 5.24.

Synthesis of 4a: The procedure is similar as for **3a**. Instead of adding H₂O₂, S₈ (38 mg, 1.2 mmol) was added. The mixture was stirred for 12 h at 50 °C. The crude residue was purified by column chromatography on silica with Petroleum ether/CH₂Cl₂ (1/1) as eluent. The product was obtained as a pale yellow solid in a 54% yield (215 mg, 0.51 mmol). ³¹P NMR (CDCl₃; 121 MHz): δ = +57.3 (s). ¹H NMR (CDCl₃; 300 MHz): δ = 7.03-7.43 (m, 18H, CHphenyl), 7.69 (d, 1H, J(H,P) = 69.9 Hz, =CH), 7.94 (ddd, 2H, J(H,P) = 14.1 Hz, J(H,H) = 7.8 Hz, J(H,H) = 1.5 Hz, CHphenyl). ¹³C NMR (CDCl₃; 75 MHz): δ = 126.8 (d, J(C,P) = 9.2 Hz, CHphenyl), 128.1 (s, CHphenyl), 128.4 (s, CHphenyl), 128.5 (s, CHphenyl), 128.6 (s, CHphenyl), 128.9 (s, CHphenyl), 129.0 (s, CHphenyl), 129.6 (s, CHphenyl), 129.9 (s, CHphenyl), 130.1 (s, CHphenyl), 130.7 (d, J(C,P) = 6.2 Hz, Cphenyl), 130.8 (d, J(C,P) = 64.8 Hz, Cipso), 131.4 (d, J(C,P) = 12.2 Hz, CHphenyl), 132.4 (d, J(C,P) = 3.0 Hz, CHphenyl), 138.6 (d, J(C,P) = 8.3 Hz, Cphenyl), 139.2 (d, J(C,P) = 16.7 Hz, Csp₂), 139.3 (s, Cphenyl), 140.2 (d, J(C,P) = 67.2 Hz, Csp₂), 143.6 (d, J(C,P) = 12.2 Hz, =CH), 153.1 (d, J(C,P) = 68.6 Hz, Csp₂). HR-MS (ESI, CHCl₃/MeOH, 50/50, v/v, m/z): [M+Na]⁺ calcd for C₂₈H₂₁SNaP, 443.09993; found 443.0999; Anal. Calcd for C₂₈H₂₁PS (420.51): C 79.98, H 5.03, S 7.63, found: C 80.01, H 5.00, S 7.66.

Synthesis of 5a: The procedure is similar as for **3a**. Instead of adding H₂O₂, (tht)AuCl (256 mg, 0.8 mmol) was added and stirred for 1 h. After solvent evaporation, crude residue was purified by column chromatography on silica with Petroleum ether/CH₂Cl₂ (2/1) as eluent. Possible further purification via crystallization in CH₂Cl₂/hexane. The product was obtained as pale yellow crystals in a 34% yield (203 mg, 0.32 mmol). ³¹P NMR (CDCl₃; 121 MHz): δ = +49.6 (s). ¹H NMR (CDCl₃; 300 MHz): δ = 7.07-7.42 (m, 18H, CHphenyl), 7.61 (ddd, 2H, J(H,P) = 14.1 Hz, J(H,H) = 8.7 Hz, J(H,H) = 1.5 Hz, CHphenyl), 7.67 (d, 1H, J(H,P) = 51.6 Hz, =CH). ¹³C NMR (CDCl₃; 75 MHz): δ = 126.3 (d, J(C,P) = 8.9 Hz, CHphenyl), 127.7 (d, J(C,P) = 43.9 Hz, Cipso), 128.4 (s, CHphenyl), 128.9 (s, CHphenyl), 129.0 (d, J(C,P) = 12.8 Hz, CHphenyl), 129.2 (s, CHphenyl), 129.4 (d, J(C,P) = 11.9 Hz, CHphenyl), 129.6 (s, CHphenyl), 129.8 (s, CHphenyl), 130.3 (s, CHphenyl), 130.8 (d, J(C,P) = 7.3 Hz, Cphenyl), 130.9 (d, J(C,P) = 57.4 Hz, Cipso), 133.3 (s, CHphenyl), 133.4 (d, J(C,P) = 14.3 Hz, CHphenyl), 138.3 (d, J(C,P) = 14.1 Hz, Csp₂), 138.4 (d, J(C,P) = 7.5 Hz, Cphenyl), 141.4 (s, Cphenyl), 143.0 (d, J(C,P) = 7.2 Hz, =CH), 147.5 (d, J(C,P) = 52.1 Hz, Csp₂). HR-MS (ESI, CH₃OCH₃, m/z): [M+Na]⁺ calcd for C₂₈H₂₁ClAuNaP, 643.06327; found 643.0632; Anal. Calcd for C₂₈H₂₁AuClP (620.87): C 54.17, H 3.41, found: C 54.49, H 3.28.

Synthesis of 3b: The procedure is similar as for **3a**. The crude residue was purified by column chromatography on silica (petroleum ether/AcOEt, 1/1) and recrystallization in absolute ethanol permit to afford product in a 45% yield (200 mg, 0.43 mmol). ³¹P NMR (CDCl₃; 121 MHz): δ = 34.4 (s). ¹H NMR (CDCl₃; 300 MHz): δ = 3.69 (s, 3H, OCH₃), 3.70 (s, 3H, OCH₃), 6.73 (d, 2H, J(H,H) = 8.7 Hz, CHphenyl), 6.79 (d, 2H, J(H,H) = 8.4 Hz, CHphenyl), 7.30-7.43 (m, 12H, CHphenyl), 7.70 (d, 1H, J(H,P) = 71.4 Hz, =CH), 7.88 (dd, 2H, J(H,P) = 11.4 Hz, J(H,H) = 7.5 Hz, CHphenyl). ¹³C NMR (CDCl₃; 75 MHz): δ = 55.2 (s, OCH₃), 55.3 (s, OCH₃), 113.8 (s, CHphenyl), 114.5 (s, CHphenyl), 123.9 (d, J(C,P) = 6.0 Hz, Cphenyl), 128.1 (s, CHphenyl), 128.5 (s,

CHphenyl), 128.7 (d, J(C,P) = 9.0 Hz, CHphenyl), 129.0 (d, J(C,P) = 12 Hz, CHphenyl), 129.9 (s, CHphenyl), 130.2 (s, CHphenyl), 130.8 (d, J(C,P) = 86.3 Hz, Cipso), 131.2 (d, J(C,P) = 11.3 Hz, CHphenyl), 132.0 (d, J(C,P) = 9.0 Hz, Cphenyl), 132.4 (d, J(C,P) = 3.0 Hz, CHphenyl), 138.4 (d, J(C,P) = 1.5 Hz, Cphenyl), 139.7 (d, J(C,P) = 17.3 Hz, Csp₂), 140.2 (d, J(C,P) = 77.3 Hz, Csp₂), 142.3 (d, J(C,P) = 12.0 Hz, =CH), 154.1 (d, J(C,P) = 78.0 Hz, Csp₂), 159.7 (s, Cphenyl), 160.8 (s, Cphenyl). HR-MS (ESI, CHCl₃/MeOH, 50/50, v/v, m/z): [M+Na]⁺ calcd for C₃₀H₂₅O₃NaP, 487.1439; found 487.1440; Anal. Calcd for C₃₀H₂₅O₃P (464.49): C 77.57, H 5.43, found: C 77.50, H 5.30.

Synthesis of 3c: The procedure is similar as for **3a**. The crude residue was purified by column chromatography on silica with dichloromethane as eluent. Product was obtained as a yellow solid in a 35% yield (180 mg, 0.33 mmol). ³¹P NMR (CDCl₃; 121 MHz): δ = +35.4 (s). ¹H NMR (CDCl₃; 300 MHz): δ = 7.20-7.23 (m, 2H, CHphenyl), 7.35-7.47 (m, 14H, CHphenyl), 7.75 (ddd, 2H, J(H,P) = 12.6 Hz, J(H,H) = 6.9 Hz, J(H,H) = 1.8 Hz, CHphenyl), 7.90 (d, 1H, J(H,P) = 69.0 Hz, =CH). ¹³C NMR (CDCl₃; 75 MHz): δ = 123.7 (q, J(C,F) = 270.5 Hz, CF₃), 123.9 (q, J(C,F) = 270.5 Hz CF₃), 125.4 (q, J(C,F) = 3.5 Hz, CHphenyl), 126.0 (q, J(C,F) = 3.8 Hz, CHphenyl), 127.4 (d, J(C,P) = 8.6 Hz, CHphenyl), 128.8 (s, CHphenyl), 128.9 (s, CHphenyl), 129.3 (d, J(C,P) = 12.2 Hz, CHphenyl), 129.4 (s, CHphenyl), 129.8 (s, CHphenyl), 130.3 (q, J(C,F) = 32.2 Hz, Cphenyl), 130.6 (d, J(C,P) = 86.1 Hz, Cipso), 131.2 (d, J(C,P) = 11.4 Hz, CHphenyl), 131.4 (q, J(C,F) = 32.5 Hz, Cphenyl), 133.0 (d, J(C,P) = 2.8 Hz, CHphenyl), 134.0 (d, J(C,P) = 6.0 Hz, Cphenyl), 138.4 (d, J(C,P) = 16.4 Hz, Csp₂), 140.2 (s, Cphenyl), 142.6 (d, J(C,P) = 8.2 Hz, Cphenyl), 143.5 (d, J(C,P) = 76.5 Hz, Csp₂), 146.7 (d, J(C,P) = 11.8 Hz, =CH), 155.3 (d, J(C,P) = 78.5 Hz, Csp₂). HR-MS (ESI, CHCl₃/MeOH, 50/50, v/v, m/z): [M+Na]⁺ calcd for C₃₀H₁₉OF₃NaP, 563.09754; found 563.0977; Anal. Calcd for C₃₀H₁₉OF₃P (540.446): C 66.67, H 3.54, found: C 66.81, H 3.40.

Synthesis of 3d: The procedure is similar as for **3a**. The crude residue was purified by column chromatography on silica with Petroleum ether/AcOEt (3/1, v/v) as eluent. Product was obtained as a yellow solid ((278 mg, 0.44 mmol, 46%). ³¹P NMR (CDCl₃; 121 MHz): δ = +36.0 (s). ¹H NMR (CDCl₃; 300 MHz): δ = 1.46 (s, 3H, CH₃), 1.49 (s, 3H, CH₃), 1.53 (s, 3H, CH₃), 1.56 (s, 3H, CH₃), 7.19 (d, 1H, J(H,H) = 8.1 Hz, CHaromatic), 7.27-7.73 (m, 20H, CHaromatic), 7.99 (d, 1H, J(H,P) = 70.8 Hz, =CH), 8.01-8.07 (m, 3H, CHaromatic). ¹³C NMR (CDCl₃; 75 MHz): δ = 26.9 (s, CH₃), 27.0 (s, CH₃), 27.1 (s, CH₃), 27.2 (s, CH₃), 46.9 (s, Cfluorenyl), 47.0 (s, Cfluorenyl), 119.7 (s, CHaromatic), 120.3 (s, CHaromatic), 120.5 (s, CHaromatic), 120.6 (s, CHaromatic), 120.9 (d, J(C,P) = 9.5 Hz, CHaromatic), 122.7 (s, CHaromatic), 123.2 (s, CHaromatic), 126.8 (d, J(C,P) = 8.6 Hz, CHaromatic), 127.1 (s, CHaromatic), 127.3 (s, CHaromatic), 127.6 (s, CHaromatic), 128.1 (s, CHaromatic), 128.3 (s, CHaromatic), 128.6 (s, CHaromatic), 128.7 (s, CHaromatic), 129.1 (d, J(C,P) = 12.0 Hz, CHaromatic), 130.2 (s, CHaromatic), 130.9 (d, J(C,P) = 83.4 Hz, Cipso), 131.4 (d, J(C,P) = 11.3 Hz, CHaromatic), 132.5 (s, CHaromatic²), 138.3 (s, Caromatic), 138.5 (d, J(C,P) = 8.6 Hz, Caromatic), 138.7 (s, Caromatic), 139.6 (s, Caromatic), 139.8 (d, J(C,P) = 16.9 Hz, Caromatic), 140.1 (s, Caromatic), 141.2 (s, Caromatic), 141.7 (d, J(C,P) = 77.0 Hz, Csp₂), 144.0 (d, J(C,P) = 12.4 Hz, =CH), 154.1 (d, J(C,P) = 8.0 Hz, Caromatic), 154.4 (s, Caromatic), 155.6 (d, J(C,P) = 78.5 Hz, Csp₂), 1 CHaromatic and 3 Caromatic are not observed, may overlap. HR-MS (ESI, CHCl₃/MeOH, 50/50, v/v, m/z): [M+Na]⁺ calcd for C₄₆H₃₇ONaP, 659.24797; found 659.2476. Anal. Calcd for C₄₆H₃₇OP (636.76): C 86.77, H 5.86, found: C 86.59, H 5.67.

Synthesis of 3e: The procedure is similar as for **3a**. The crude product was purified by chromatography on silica (Petroleum ether/AcOEt, 2/1). The recovered fraction was crystallized in Et₂O and hexane to get a yellow solid (277 mg, 0.55 mmol, 58% yield). ³¹P NMR (CDCl₃; 121 MHz): δ = +36.4 (s). ¹H NMR (CDCl₃; 300 MHz): δ = 7.03-7.71 (m, 23H, CHaromatic), 8.49 (d, 1H, J(H,P) = 72.0 Hz, =CH), 8.63 (d, 1H, J(H,H) = 8.4 Hz, CHaromatic). ¹³C NMR (CDCl₃; 100 MHz): δ = 125.4 (s, CHaromatic), 125.6 (s, CHaromatic), 125.8 (s, CHaromatic), 126.1 (s, CHaromatic), 126.2 (s, CHaromatic), 126.6 (s, CHaromatic), 127.5 (d, J(C,P) = 9.4 Hz, CHaromatic), 127.7 (s, CHaromatic), 128.3 (s, CHaromatic), 128.5 (s, CHaromatic), 128.6 (s, CHaromatic), 128.7 (s, CHaromatic), 128.8 (s, CHaromatic), 128.9 (s, CHaromatic), 129.0 (s, CHaromatic),

129.1 (s, CHaromatic), 129.5 (d, J(C,P) = 3.6 Hz, Caromatic), 130.6 (d, J(C,P) = 79.8 Hz, C_{ipso}), 130.7 (s, CHaromatic), 131.1 (d, J(C,P) = 11.6 Hz, CHaromatic), 131.7 (s, Caromatic), 132.3 (s, CHaromatic), 133.9 (s, Caromatic), 134.1 (s, Caromatic), 136.8 (d, J(C,P) = 10.7 Hz, Caromatic), 138.5 (s, Caromatic), 140.0 (d, J(C,P) = 17.5 Hz, Csp₂), 144.7 (d, J(C,P) = 82.1 Hz, Csp₂), 146.5 (d, J(C,P) = 12.5 Hz, =CH), 157.2 (d, J(C,P) = 73.4 Hz, Csp₂), One Caromatic are not observed, may overlap. HR-MS (ESI, MeOH, *m/z*): [M+Na]⁺ calcd for C₃₆H₂₅OPNa, 527.15407; found 527.1538; Anal. Calcd for C₃₆H₂₅OP (504.16): C 85.70, H 4.99, found: C 85.95, H 5.24.

Synthesis of 3f: The procedure is similar as for **3a**. The crude product was purified by chromatography on silica (Petroleum ether/AcOEt, 4/1, v/v). The recovered fraction was crystallized in Et₂O and hexane to get a yellow solid (315 mg, 0.44 mmol, 46% yield). ³¹P NMR (CDCl₃; 121 MHz): δ = + 34.6 (s). ¹H NMR (CDCl₃; 300 MHz): ¹H NMR (CDCl₃; 300 MHz): δ = 0.85 (t, 3H, J(H,H) = 6.6 Hz, CH₃), 0.87 (t, 3H, J(H,H) = 6.6 Hz, CH₃), 1.31-1.35 (m, 8H, CH₂), 1.81-1.83 (m, 4H, CH₂), 4.22 (t, 4H, J(H,H) = 7.2 Hz, N-CH₂), 7.13-7.59 (m, 18H, CH_{aromatic}), 7.80 (s, 1H, CH_{aromatic}), 7.90 (d, 1H, J(H,P) = 71.7 Hz, =CH) 7.97-8.18 (m, 5H, CH_{aromatic}). ¹³C NMR (CDCl₃; 75 MHz): δ = 13.9 (s, CH₃), 13.9 (s, CH₃), 22.4 (s, CH₂), 22.5 (s, CH₂), 28.6 (s, CH₂), 28.7 (s, CH₂), 29.3 (s, CH₂), 29.4 (s, CH₂), 43.2 (s, 2CH₂), 108.5 (s, CHaromatic), 108.7 (s, CHaromatic), 109.0 (s, CHaromatic), 109.2 (s, CHaromatic), 118.9 (s, CHaromatic), 119.5 (s, CHaromatic), 119.6(s, CHaromatic), 120.7(s, CHaromatic), 120.8 (s, CHaromatic), 121.3 (s, CHaromatic), 122.5 (d, J(C,P) = 6.0 Hz, Caromatic), 122.7 (s, Caromatic), 122.8 (s, Caromatic), 123.0 (s, Caromatic), 123.3 (s, Caromatic), 125.0 (d, J(C,P) = 9.2 Hz, CHaromatic), 125.7 (s, CHaromatic), 126.2 (s, CHaromatic), 127.2 (s, CHaromatic), 127.9 (s, CHaromatic), 128.5 (s, CHaromatic), 129.0 (d, J(C,P) = 11.9 Hz, CHaromatic), 130.3 (s, CHaromatic), 130.8 (d, J(C,P) = 8.8 Hz, Caromatic), 131.5 (d, J(C,P) = 11.2 Hz, CHaromatic), 131.7 (d, J(C,P) = 83.5 Hz, C_{ipso}), 132.2 (s, CHaromatic), 138.9 (s, Caromatic), 140.4 (s, Caromatic), 140.5 (d, J(C,P) = 80.1 Hz, Csp₂), 140.6 (d, J(C,P) = 17.3 Hz, Csp₂), 140.8 (s, Caromatic), 141.0 (s, Caromatic), 141.9 (d, J(C,P) = 12.9 Hz, =CH), 155.2 (d, J(C,P) = 78.1 Hz, Csp₂). One Caromatic are not observed, may overlap. HR-MS (ESI, CH₂Cl₂/MeOH, 10/90, v/v, *m/z*): [M+Na]⁺ calcd for C₅₀H₄₇ON₂PNa, 745.33182; found 745.3316; Anal. Calcd for C₅₀H₄₇ON₂P (722.34): C 83.07, H 6.55, found: C 83.25, H 6.24.

Acknowledgements

This work is supported by the Ministère de la Recherche et de l'Enseignement Supérieur, the Institut Universitaire de France, the CNRS, the Région Bretagne, China-French associated international laboratory in "Functional Organophosphorus Materials" and COST CM0802 (Phoscinet). National Natural Science Foundation (21072179, 21272218) of China, Henan Science and Technology Department (114300510007), and Zhengzhou Science and Technology Department (131PYSGGZ204). The authors are grateful to C. Lescop for X-ray diffraction studies and to J. Troles for the DSC measurements. (Supporting Information is available online from Wiley InterScience or from the author).

- [1] a) C. W. Tang, S. A. VanSlyke, *Appl. Phys. Lett.* **1987**, *51*, 913; b) C. Adachi, S. Tokito, T. Tsutsui, S. Saito, *Jpn J. Appl. Phys.* **1988**, *27*, 1269; c) C. W. Tang, S. A. VanSlyke, C. H. Chen, *J. Appl. Phys.* **1989**, *65*, 3610; d) B. W. D'Andrade, S. R. Forrest, *Adv. Mater.* **2004**, *16*, 1585; e) K. T. Kamtekar, A. P. Monkman, M. R. Bryce, *Adv. Mater.* **2010**, *22*, 572; f) B. W. D'Andrade, *Nat. Photonics.* **2007**, *1*, 33; g) M. C. Gather, A. Köhnen, K. Meerholz *Adv. Mater.* **2011**, *23*, 233.
- [2] a) P.-A. Bouit, A. Escande, R. Szűcs, D. Szieberth, C. Lescop, L. Nyulászi, M. Hissler, R. Réau, *J. Am. Chem. Soc.* **2012**, *134*, 6524; b) Y. Ren, W. H. Kan, M. A. Henderson, P. G. Bomben, C. P. Berlinguette, V. Thangadurai, T. Baumgartner, *J. Am. Chem. Soc.* **2011**, *133*, 17014; c) E. Deschamps, L. Ricard, F. Mathey *Angew. Chem. Int. Ed. Engl.* **1994**, *33*, 1158; d) Y. Matano, M. Nakashima, H. Imahori, *Angew. Chem. Int. Ed.* **2009**, *48*, 4002; e) K. Yavari, S.

- Moussa, B. Ben Hassine, P. Retailleau, A. Voituriez, A. Marinetti, *Angew. Chem. Int. Ed.* **2012**, *51*, 6748; f) W. Weymiens, M. Zaal, J. C. Slootweg, A. W. Ehlers, K. Lammertsma *Inorg. Chem.* **2011**, *50*, 8516; g) Y. Dienes, M. Eggenstein, T. Kárpáti, T. C. Sutherland, L. Nyulászi, T. Baumgartner, *Chem. Eur. J.* **2008**, *14*, 9878; h) A. Fukazawa, M. Hara, T. Okamoto, E.-C. Son, C. Xu, K. Tamao, S. Yamaguchi, *Org. Lett.* **2008**, *10*, 913; i) A. Fukazawa, H. Yamada, S. Yamaguchi, *Angew. Chem. Int. Ed.* **2008**, *47*, 5582.
- [3] a) H. Chen, W. Delaunay, L. Yu, D. Joly, Z. Wang, J. Li, Z. Wang, C. Lescop, D. Tondelier, B. Geffroy, Z. Duan, M. Hissler, F. Mathey, R. Réau, *Angew. Chem. Int. Ed.* **2012**, *51*, 214; b) D. Joly, D. Tondelier, V. Deborde, W. Delaunay, A. Thomas, K. Bhanuprakash, B. Geffroy, M. Hissler, R. Réau *Adv. Funct. Mater.* **2012**, *22*, 567; c) D. Joly, D. Tondelier, V. Deborde, B. Geffroy, M. Hissler, R. Réau *New. J. Chem.*, **2010**, *8*, 1603; d) O. Fadhel, M. Gras, N. Lemaître, V. Deborde, M. Hissler, B. Geffroy, R. Réau *Adv. Mat.*, **2009**, *21*, 1261; e) H. Su, O. Fadhel, C.-J. Yang, T.-Y. Cho, C. Fave, M. Hissler, C.-C. Wu, R. Réau, *J. Am. Chem. Soc.*, **2006**, *128*, 983.
- [4] Phosphorus-Carbon Heterocyclic chemistry : the rise of a new domain, ed F. Mathey, Pergamon 2001
- [5] a) A. Marinetti, J. Fischer, F. Mathey, *J. Am. Chem. Soc.* **1985**, *107*, 5001; b) N. H. Tran Huy, L. Richard, F. Mathey, *Organometallics* **1988**, *7*, 1791; c) H. Jun, R. J. Angelici, *Organometallics* **1993**, *12*, 4265; d) L. Weber, O. Kaminski, H.-G. Stammer, B. Neumann, *Organometallics* **1995**, *14*, 581; e) L. Dupuis, N. Pirio, P. Meunier, A. Igau, B. Donnadiou, J.-P. Majoral, *Angew. Chem. Int. Ed.* **1997**, *36*, 987; f) N. Pirio, S. Bredeau, L. Dupuis, P. Schütz, B. Donnadiou, A. Igau, J.-P. Majoral, J.-C. Guillemin, P. Meunier, *Tetrahedron* **2004**, *60*, 1317; g) M. Zablocka, J. M. Majoral, *Current Org. Chem.*, **2007**, *11*, 49.
- [6] a) A. Hengefeld, R. Nast, *Chem. Ber.* **1983**, *116*, 2035; b) I. P. Beletskaya, V. V. Afanasiev, M. A. Kazankova, I. V. Efimova, *Org. Lett.* **2003**, *23*, 4309; c) V. V. Afanasiev, I. P. Beletskaya, M. A. Kazankova, I. V. Efimova, M.-U. Antipin, *Synthesis* **2003**, *18*, 2835.
- [7] M. A. A. El Bayoumi, F. M. A. Halim *J. Chem. Phys.* **1968**, *48*, 2536.
- [8] a) N. Matsusue, S. Ikame, Y. Suzuki, H. Naito, *Appl. Phys. Lett.*, **2004**, *85*, 4046. b) H. I. Baek, C. Lee, *J. Appl. Phys.* **2008**, *103*, 054510.
- [9] a) H. Choukri, A. Fischer, S. Forget, S. Chénais, M.-C. Castex, D. Adès, A. Siove, B. Geffroy, *Appl. Phys. Lett.* **2006**, *89*, 183513. b) E.I. Haskal, *Synthetic Metals* **1997**, *91*, 157.
- [10] J. N. Demas, G. A. Crosby, *J. Phys. Chem.* **1971**, *75*, 991.
- [11] Z. Otwinowski, W. Minor In *Methods in Enzymology*, (Ed.: C.W. Carter, Jr. & R.M. Sweet), New York:Academic Press, **1997**, *276*, 307.
- [12] A. Altomare, M.C. Burla, M. Camalli, G. Cascarano, C. Giacovazzo, A. Guagliardi, A. G. G. Moliterni, G. Polidori, R. Spagna, *J. of Applied Cryst.* **1999**, *32*, 115
- [13] International Tables for X-ray Crystallography, vol C, Ed. Kluwer, Dordrech, **1992**
- [14] Gaussian 03, Revision C.02, M. J. Frisch, G. W. Trucks, H. B. Schlegel, G. E. Scuseria, M. A. Robb, J. R. Cheeseman, J. A. Montgomery, Jr., T. Vreven, K. N. Kudin, J. C. Burant, J. M. Millam, S. S. Iyengar, J. Tomasi, V. Barone, B. Mennucci, M. Cossi, G. Scalmani, N. Rega, G. A. Petersson, H. Nakatsuji, M. Hada, M. Ehara, K. Toyota, R. Fukuda, J. Hasegawa, M. Ishida, T. Nakajima, Y. Honda, O. Kitao, H. Nakai, M. Klene, X. Li, J. E. Knox, H. P. Hratchian, J. B. Cross, C. Adamo, J. Jaramillo, R. Gomperts, R. E. Stratmann, O. Yazyev, A. J. Austin, R. Cammi, C. Pomelli, J. W. Ochterski, P. Y. Ayala, K. Morokuma, G. A. Voth, P. Salvador, J. J. Dannenberg, V. G. Zakrzewski, S. Dapprich, A. D. Daniels, M. C. Strain, O. Farkas, D. K. Malick, A. D. Rabuck, K. Raghavachari, J. B. Foresman, J. V. Ortiz, Q. Cui, A. G. Baboul, S. Clifford, J. Cioslowski, B. B. Stefanov, G. Liu, A. Liashenko, P. Piskorz, I. Komaromi, R. L. Martin, D. J. Fox, T. Keith, M. A. Al-Laham, C. Y. Peng, A. Nanayakkara, M. Challacombe, P. M. W. Gill, B. Johnson, W. Chen, M. W. Wong, C. Gonzalez, and J. A. Pople, Gaussian, Inc., Wallingford CT, 2004

[15] a) A. Hengefeld, R. Nast, *Chem. Ber.* **1983**, *116*, 2035; b) I. P. Beletskaya, V. V. Afanasiev, M. A. Kazankova, I. V. Efimova, *Org. Lett.* **2003**, *23*, 4309; c) V. V. Afanasiev, I. P. Beletskaya, M. A. Kazankova, I. V. Efimova, M.-U. Antipin,

Synthesis **2003**, *18*, 2835.

